ELSEVIER

On the essential work of fracture of neat and rubber toughened polyamide-66

Alessandro Pegoretti [a,*], Theonis Ricco [b]

[a] *Department of Materials Engineering and Industrial Technologies and INSTM Research Unit, University of Trento,*
via Mesiano 7, 38050 Trento, Italy
[b] *Department of Chemistry and Physics for Engineering and Materials and INSTM Research Unit, University of Brescia,*
via Valotti 9, 25123 Brescia, Italy

Abstract

Essential work of fracture (EWF) tests have been conducted on neat and rubber toughened polyamide-66 in order to measure the essential specific work of fracture (w_e) and the non-essential specific work of fracture (βw_p) parameters. Further, the w_e value has been partitioned into two terms, one related to the specific energy contribution for yielding up to the onset of fracture ($w_{e,init}$), and another one representing the subsequent crack propagation process ($w_{e,prop}$), respectively. EWF tests performed on neat polyamide-66 specimens conditioned up to various equilibrium moisture contents clearly indicate that w_e markedly increases as the material moisture content rises, and that this trend is mainly associated with the increase of its crack propagation component ($w_{e,prop}$), the initiation related term ($w_{e,init}$) being practically independent of the humidity level. The inclusion of various amounts (7, 16, and 25 wt%) of rubber particles (a random ethylene–acrylic ester–maleic anhydride terpolymer) into the polyamide-66 matrix induces a large increase of the w_e parameter. It is interesting to observe that the $w_{e,init}$ and $w_{e,prop}$ terms display different trends with the rubber content. Most of the toughening effect of the rubber particles can be attributed to a large increase of the propagation-related term, the fracture initiation term decreasing with the rubber content. Finally, the loading rate effects on the fracture behaviour have been investigated for polyamide-66 toughened with 25 wt% rubber. An increase of the loading rate causes an increase of the crack-initiation related term $w_{e,init}$, while the crack-propagation related parameter $w_{e,prop}$ decreases. As a consequence, the specific term w_e shows a non-monotonic trend with the loading rate.
© 2006 Elsevier Ltd. All rights reserved.

Keywords: Essential work of fracture; Polyamide-66; Rubber-toughening; Strain rate effects

1. Introduction

Rubber-toughening of plastics requires the inclusion of discrete rubbery phases within the polymer to be toughened, typically in the form of micron or sub-micron size particles at volume fractions in the range

---

* Corresponding author. Tel.: +39 0461 882452; fax: +39 0461 881977.
E-mail address: alessandro.pegoretti@ing.unitn.it (A. Pegoretti).

0.05–0.30 [1,2]. Nowadays it is well established that the toughening effect achieved through introduction of dispersed rubbery particles comes principally from the increase in fracture energy related to the yielding of the polymer matrix, the role of the rubbery particles being simply to induce yielding processes in the matrix [1–4]. Polyamides constitute a commercially important class of engineering polymers [5] and a great deal of efforts have been expended over the last twenty years in the development of effective rubber-toughened blends [6–21]. The most important parameters in the rubber-toughening of polyamides are (i) the rubber content, (ii) the average particle size and its distribution, (iii) the type of rubber, (iv) the distribution of the rubber particles, (v) the level of particle–matrix adhesion, whose effects are exhaustively examined in the review articles of Gaymans [22] and Keskkula and Paul [23]. In most cases, the toughening effects of rubber addition to polyamides have been mainly studied by simple Charpy and Izod tests on notched specimens [22,23]. On the other hand, the use of rigorous fracture mechanics methodologies to quantify the effects of rubber addition on the fracture behaviour of polyamides is quite limited in the scientific literature [9,19–21,24,25]. The main reason is that the testing methods successfully developed in the framework of the linear elastic fracture mechanics (LEFM) for brittle polymers can be hardly applied for rubber toughened engineering plastics. In fact, LEFM conditions require linear load–displacement behaviour and very localized deformation at the crack tip [26]. The latter condition implies that the radius of the plastic zone at the crack tip has a negligible effect on the stress around the crack tip and thus on the measured critical values of plane-strain fracture toughness (K_{IC}) or strain energy release rate (G_{IC}). Thus, the specimens size requirements for LEFM testing methods limit the size of the crack tip plastic zone relative to the specimens dimensions [27,28] as follows:

$$B, a, (W - a) > 2.5 \left(\frac{K_{IC}}{\sigma_y} \right)^2 = 2.5 \frac{E G_{IC}}{(1 - v^2) \sigma_y^2} \tag{1}$$

where B is the specimen thickness, W its width, a is the initial crack length, σ_y is the material yield strength, E is the Young's modulus, and v is the Poisson's ratio at the temperature and strain rate of the fracture test. For rubber-toughened blends the condition expressed by Eq. (1) requires testing on very thick specimens, that cannot be formed easily by injection moulding, and elastic–plastic fracture mechanics (EPFM) methods [29] have to be applied. The most common EPFM method is based on the evaluation of J_{IC} that represents a critical value of the J-contour integral. The validity criteria for the specimen thickness for J_{IC} is

$$B > 25 \left(\frac{J_{IC}}{\sigma_y} \right) \tag{2}$$

which is about a factor of five less than Eq. (1) [29]. The J-integral method alleviates to some degree the stringent size requirements of LEFM, however, the thickness required is still often beyond what can be conveniently injection moulded [18]. Moreover, the recommended procedure for measuring J_{IC}, based on a multiple specimens R-curve method [30,31], requires the evaluation of the crack advancement on the partially fractured specimens. This procedure is quite time consuming and needs the use of several specimens. For the above mentioned reasons, even if some attempts have been made to simplify the procedure [24], this method has been rarely applied to characterize the fracture behaviour of rubber toughened polyamides [9,24,25].

The essential work of fracture (EWF) method is an alternative, less time consuming, EPFM approach that has been extensively used for the fracture toughness assessment of ductile polymeric materials under plane stress conditions [29,32]. This method has been recently applied to the fracture characterization of both neat [33–35] and rubber toughened polyamides [19–21]. Further, the EWF method has also been successfully used for the fracture characterization of rubber toughened polyamides reinforced with glass fibers [36–43] or montmorillonite [44].

In this study the essential work of fracture (EWF) approach has been adopted to investigate the fracture behaviour of neat and rubber toughened polyamide-66 sheets. The objective of the work is to analyse the effects of (i) the moisture content, (ii) the rubber content, and (iii) the strain rate, on the essential work of fracture parameters of the selected materials.

2. Experimental

2.1. Materials and specimens conditioning

The polymer matrix used in this research is a commercial neat polyamide-66 (Radilon-HS100). Three rubber toughened grades (Radilon-HSX, Radilon-ESL128, Radilon-USX200) based on this matrix and containing 7, 16 and 25 wt% of rubber particles, respectively, have been also used [45]. The rubber is a random ethylene–acrylic ester–maleic anhydride terpolymer (Lotader®MAH). All the materials were kindly supplied by Radici Novacips SpA (Villa d'Ogna, Bergamo, Italy) as injection moulded square plaques of $60 \times 60 \times 1$ mm^3 and as ISO 527-1A [46] dumb-bell tests pieces. The barrel and nozzle temperature were kept at 280 °C, the injection pressure was 40 bar and the mould temperature was 50 °C. Before being used, all the specimens had been stored for two months under laboratory conditions ($T = 21$ °C, RH = 30%) until a constant weight was reached.

In order to investigate the effect of water on the fracture behaviour, some of the neat polyamide-66 plaques were dried under vacuum at 80 °C for 36 h (dry specimens). Half of this sample was then allowed to equilibrate its moisture content under laboratory conditions ($T = 21$ °C, RH = 30%) until a constant weight was reached (moisture uptake of 1.3 wt%). The second half was immersed in distilled water at 70 °C for 72 h (moisture uptake of 9.3 wt%).

In order to levelling off any orientation-related effect, all the experiments have been performed on specimens obtained along the same direction in the moulded plaques.

2.2. Analysis of rubber particles

Rectangular strips ($40 \times 4 \times 1$ mm^3) were machined out from the injection moulded plaques, immersed for 30 min in liquid nitrogen and broken under impact conditions. The broken surfaces were etched in xylene at 80 °C for 30 min and the solvent was allowed to evaporate for 12 h under an extractor hood. The fracture surfaces were sputtered with gold and observed with a scanning electron microscope (SEM) Cambridge model Stereoscan 200. Observations were made at an accelerating voltage of 20 kV.

The analysis of the rubber particles was performed by a semi-automatic digital image analysis technique which employed ImageJ 1.34S software developed and freely distributed by the National Institute of Heath of USA. The apparent diameter was determined by scanning the SEM micrographs and individually measuring the particle dimension as an average of their longest dimension and the dimension perpendicular to the major axis. Typically over 250 particles were analysed for each blend composition.

Moreover the particle density was assessed by counting the number of particles in a representative area of about 100 μm^2.

2.3. Dynamic mechanical thermal analysis

Dynamic mechanical thermal analysis (DMTA) tests were conducted in a tensile loading mode, by a Polymer Laboratories dynamic mechanical thermal analyser (model MkII) on rectangular strips having the same dimensions of those used for the analysis of rubber particles. All measurements were performed with a peak to peak displacement of 32 μm, in a temperature range from −150 °C up to 240 °C, at a heating rate of 3 °C/min and at a frequency of 1 Hz.

2.4. Tensile test

In order to obtain information on the uniaxial tensile properties of the injection moulded plaques, specimens for tensile tests were punch-cut from them according to the 1BA dumb-bell geometry described in the ISO 527 standard [46]. Tensile tests were performed by an Instron model 4502 universal testing machine equipped with a 1 kN load cell, on at least five specimens. Deformation up to 0.01 was monitored by an Instron model 2620 clip-on extensometer with a gage length of 25 mm, while higher deformations were

monitored by the cross-head displacement. The tests were performed at room temperature and at various cross-head speeds from 10 to 500 mm/min.

2.5. Charpy impact test

Charpy impact tests were performed by a CEAST model 6549 instrumented pendulum according to ISO 179 standard [47]. Rectangular specimens 10 mm wide, 80 mm long, and 4 mm thick were machined from the injection moulded dumb-bell samples. A notch type 1eA (radius of notch base of 0.25 mm, ligament 8 mm) was obtained with a milling machine. The specimen were tested in the edgewise direction supported at a span length of 62 mm. The striking nose of the pendulum is characterized by an included angle of 30° and the tip is rounded to a radius of 2 mm. All impact test were performed at a striking speed of 2.83 m/s and at a impact energy of 5 J. At least five specimens were tested for each experimental condition.

2.6. Fracture toughness characterization

The EWF approach is based on the assumption that the total work of fracture, W_f, is the sum of two energy terms:

$$W_f = W_e + W_p \tag{3}$$

where W_e is the energy consumed in the fracture process zone, and W_p is the energy dissipated in the outer plastic region, where a number of energy dissipation mechanisms may occur. By assuming that W_e is proportional to the ligament area, and W_p is proportional to the volume of the outer plastic region, the following specific terms can be defined:

$$w_e = \frac{W_e}{tL}; \quad w_p = \frac{W_p}{\beta tL^2} \tag{4}$$

where w_e is the specific essential work of fracture, and w_p is the specific non-essential work of fracture, t is the specimen thickness, L is the ligament length and β is a plastic zone shape factor depending on the geometry of the specimen and the crack. By combining Eq. (4) into Eq. (3) the following relationship can be obtained:

$$w_f = \frac{W_f}{tL} = w_e + \beta w_p L \tag{5}$$

where the terms w_f, w_e and βw_p are the specific total, essential, and non-essential work of fracture, respectively.

EWF tests were performed on deeply double-edge notched tension (DDENT) specimens whose dimensions were selected on the basis of the ESIS-TC4 test protocol [32]. In particular, the initial distance between grips was chosen equal to the width and fixed at 40 mm. The ligament length was varied in order to cover the range between 5 and 15 mm. Notches were made by an automatic notching device mounting a sharpened razor blade. All the fracture tests were performed at room temperature and at various cross-head speeds in the range from 1 to 500 mm/min. Accordingly to the ESIS test protocol, a stress criterion was adopted in order (i) to ensure greater likelihood of fracture to occurring under plane stress conditions and (ii) to remove data where fracture has occurred prior to full ligament yielding. This check is based on the evaluation of a net-section stress $\sigma_{max} = P_{max}/Lt$, where P_{max} is the maximum peak load, L is the ligament length and t is the thickness of the specimen. For all the data an average value for σ_{max}, denoted by σ_m, was determined, and the specimens for which $\sigma_{max} < 0.9\sigma_m$ or $\sigma_{max} > 1.1\sigma_m$ were rejected. For each valid specimen the total energy to failure (W_f) was calculated from the load–displacement traces, a specific value (w_f) was computed according to Eq. (5), and the data plotted against L. A least square regression line was used to fit the data, and the points lying more than two times the standard deviation from the best-fit line were eliminated. Having rejected these points, a final least squares linear regression line was obtained considering the remaining data to give the intercept, which is called the essential specific work of fracture (w_e), and its slope, which is called the non-essential specific work of fracture (βw_p).

3. Results and discussion

3.1. Preliminary characterization

Fig. 1 shows the SEM micrographs of the etched fracture surfaces of neat and rubber-modified polyamide-66 specimens. For all the investigated compositions, the rubber particles appear as discrete spheroids almost homogenously dispersed in the polyamide-66 matrix. Of course, the fractured surfaces cannot always cut through the centre of each rubber particle and hence, in SEM photomicrographs, the particles appear to be smaller and more broadly distributed in size than they really are. Therefore, direct measurements on the micrographs lead to the determination of an apparent diameter d_A. The probability distributions of the apparent particle diameters are reported in Fig. 2 for the various rubber contents. It is interesting to note that, as the rubber content increases, the probability distributions shift towards higher diameter values and appear to be more and more dispersed. For randomly distributed particles, Wu [6] proposed that the true average diameter $\bar{d}_T$ is related to the apparent average diameter $\bar{d}_A$ by the following relationship:

$$\bar{d}_T = \left(\frac{4}{\pi}\right)\bar{d}_A \tag{6}$$

The true average diameter values have been estimated on the basis of Eq. (6) and reported in Table 1 together with their standard deviations. It is worthwhile to note that the average values of the particle diameter are always lower than 0.5 μm and the standard deviations increase as the rubber content increases. It is well known that the impact strength of rubber toughened polyamides does strongly depend on the particle size [22,23]. In fact, for the rubber to be effective the particle size has to be in an optimal range. For example, the impact strength values of polyamide-6 blended with 20 wt% of ethylene–propylene rubber as a function of particle size, shows that there is a lower limit of about 0.1 μm and an upper limit at about 1 μm [22,23]. No information are currently available on the effects of particle size on the essential work of fracture para-
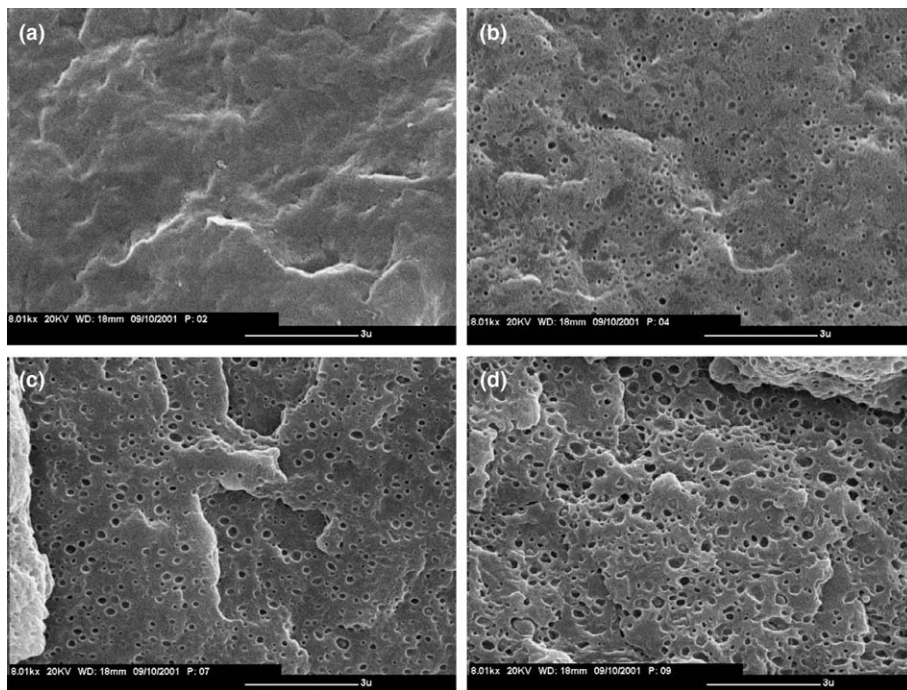
Fig. 1. Scanning electron photomicrographs of cryogenic fractured and etched surfaces of (a) neat, (b) 7 wt% rubber modified, (c) 16 wt% rubber modified, and (d) 25 wt% rubber modified polyamide-66.
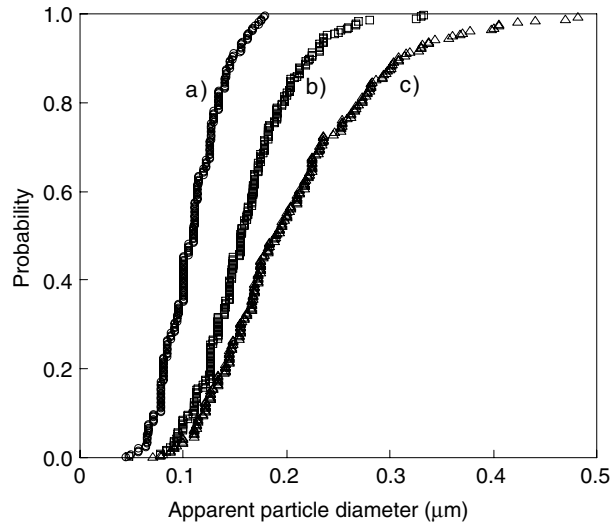
Fig. 2. Probability distributions of the apparent particle diameters for (a) 7 wt% rubber modified, (b) 16 wt% rubber modified, and (c) 25 wt% rubber modified polyamide-66.

Table 1
Average diameter and density of rubber particles in rubber modified polyamide-66

Rubber content (wt%)	Average particle diameter, $\bar{d}_T$ (nm)	Particle density (count/μm^2)
7	139 ± 37	7.29
16	205 ± 61	7.20
25	261 ± 99	7.27

meters in rubber modified polyamides. On the same Table 1, the number of particles per unit area are also reported. It is worth noting that the investigated materials contain approximately the same number of particles per unit area, independently of the rubber content.

In Fig. 3 the storage and loss factor DMTA thermograms of neat and rubber toughened polyamide-66 are reported. Neat polyamide-66 shows three loss factor peaks located at 45 °C, −72 °C and −135 °C, usually named α, β and γ damping peaks, respectively [48]. The α-damping peak, corresponding to the glass transition
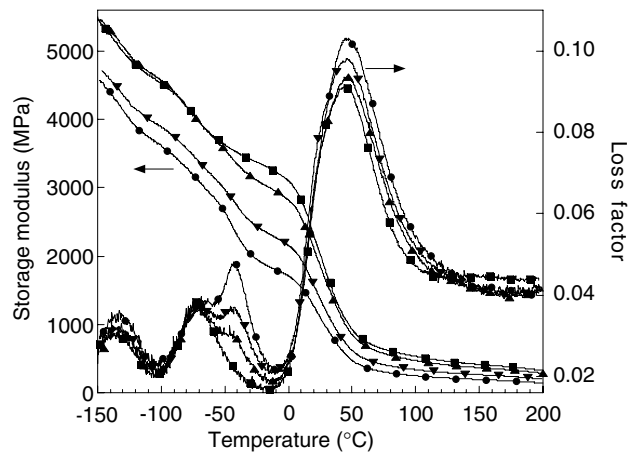
Fig. 3. Storage modulus and loss factor thermograms for (■) neat, (▲) 7 wt% rubber modified, (▼) 16 wt% rubber modified, and (●) 25 wt% rubber modified polyamide-66. Specimens conditioned at $T = 21$ °C and RH = 30%.

temperature, T_g, is of greater magnitude than the damping peaks at lower temperatures. Its origin is believed to result from the rupture of hydrogen bonds between polymeric chains, which give rise to the motion of long-chain segments in the amorphous regions. On the other hand, the origin of the β-transition is attributed to segmental motion that involves amide groups in the amorphous regions, that are not hydrogen bonded to other amides or a nearby chain. The γ-transition is thought to be associated with the small-scale reorientational motion in the amorphous region of the methylene units between amide group [49]. As evidenced in Fig. 3, the presence of rubber particles profoundly affects the dynamic-mechanical thermal behaviour of polyamide-66. In fact, the storage modulus decreases as the rubber content increases and an additional loss factor peak, located at about −43 °C, appears in the rubber toughened polyamide-66 specimens. This damping peak corresponds to the glass transition of the rubber particles, as confirmed by parallel differential scanning calorimetry measurements performed on the rubber additive. Of course, the intensity of this damping peak is directly proportional to the amount of rubber particles. The presence of rubber particles also slightly increases the intensity of the α-damping peak of the polyamide-66 matrix.

The tensile mechanical properties of neat and rubber toughened polyamide-66 at various testing speed is summarized in Fig. 4. The tensile modulus almost linearly decreases with the rubber content, being only slightly affected by the testing speed (see Fig. 4a). Borggreve et al. [8] found that for polyamide–rubber blends with a particle dispersion the modulus of the blends linearly decreased with the rubber volume fraction. For as concern the yield behaviour of the investigated materials it can be observed that, as reported in Fig. 4b, as the amount of rubber phase increases, the stress at yield decreases while the strain at yield increases. Both these parameters appear to substantially increase as the testing speed increases. Also the fracture-related parameters, reported in Fig. 4c, result to be affected by the presence of rubber particles. In fact, a certain tendency can be observed for the rubber particles to reduce the stress at break and to increase the strain at break values. The effect of the testing speed on these parameters is not so clear. In fact, opposite rate effects can be observed on the fracture behaviour of neat and 25 wt% rubber toughened polyamide-66 samples.

The load–displacement curves under Charpy impact conditions of neat and rubber toughened polyamide-66 are reported in Fig. 5. The neat polyamide-66 specimens fail in a brittle manner while the presence of rubber particles markedly modifies the failure mode towards a ductile behaviour. Table 2 summarizes the data obtained from the Charpy impact tests. As expected, the Charpy impact strength greatly increases with the rubber content. At the same time the maximum load values are always greater for the rubber modified polyamide-66 with respect to the neat matrix, but with a tendency to decrease as the rubber content increases. Beaumont et al. [50] defined a dimensionless parameter called the ductility index (DI), as the ratio between the propagation and the initiation energies. The fracture initiation point is usually considered as the point where the maximum load is reached. This parameter is found useful for ranking the impact performance of different materials under similar testing conditions, since high values of DI mean that most of the total energy is expended for crack propagation. The DI values reported in Table 2 clearly show that the presence of rubber particles markedly promotes a ductile behaviour of the investigated materials.

3.2. Fracture toughness characterization

3.2.1. Energy partitioning

A typical load–displacement curve for neat polyamide-66 DDENT specimen tested at a cross-head speed of 10 mm/min is reported in Fig. 6a together with some pictures of the ligament region taken during the fracture process. An extended whitening precedes the crack propagation process thus indicating the occurrence of yielding of the ligament region. Analysing the filmed sequence of the experiments, it has been possible to measure the crack length during the test. This information is reported in Fig. 6b, as a percentage of the ligament length. It is interesting to observe that the crack starts to propagate in correspondence of the maximum load reached during the tensile test. This experimental observation holds for all the investigated material and testing speeds. On the basis of this experimental evidence the total work of fracture W_t under the load–displacement curve can be considered as the summation of two contributes: a term $W_{f,init}$ related to the crack initiation process, and a term $W_{f,prop}$ associated to the crack propagation process, as evidenced on the same Fig. 6b. As previously proposed by other authors [51–62], the specific terms $w_{f,init}$ and $w_{f,prop}$ can be expressed as a function of the ligament length similarly to Eq. (5), as follows:

$$w_{f,init} = \frac{W_{f,init}}{tL} = w_{e,init} + \beta_{init} w_{p,init} L \tag{7a}$$

$$w_{f,prop} = \frac{W_{f,prop}}{tL} = w_{e,prop} + \beta_{prop} w_{p,prop} L \tag{7b}$$
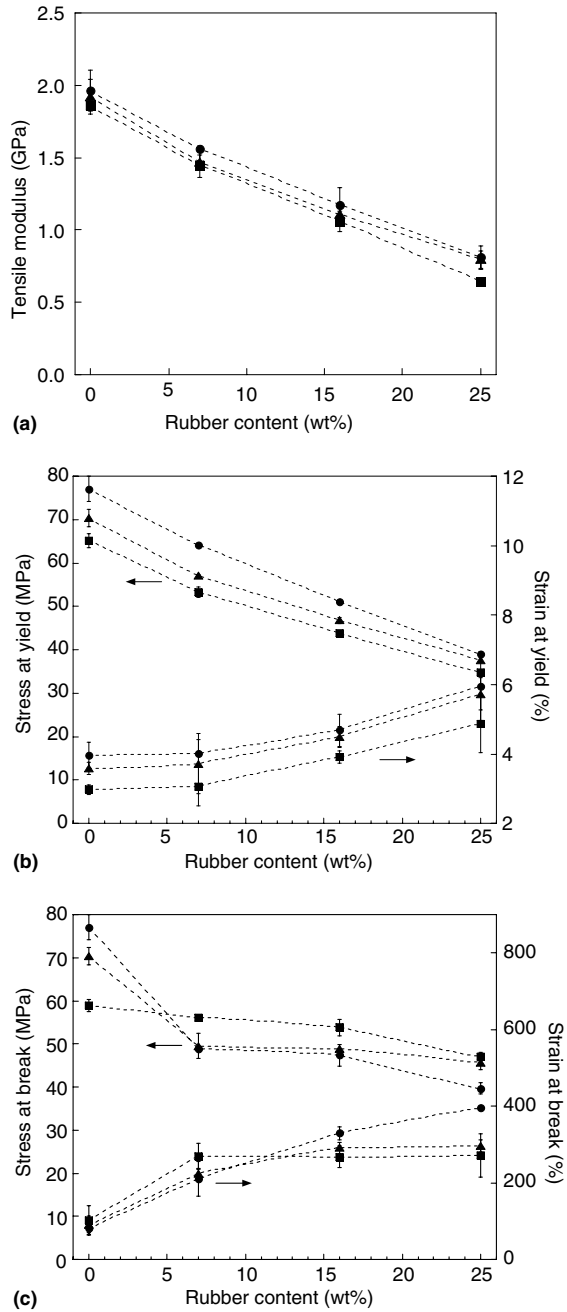
Fig. 4. Effect of rubber content on (a) tensile modulus, (b) stress and strain at yield, (c) stress and strain at break of polyamide-66 un-notched specimens tested at a cross-head speed of (■) 10 mm/min, (▲) 100 mm/min, and (●) 500 mm/min. Specimens conditioned at $T = 21\,°C$ and $RH = 30\%$.
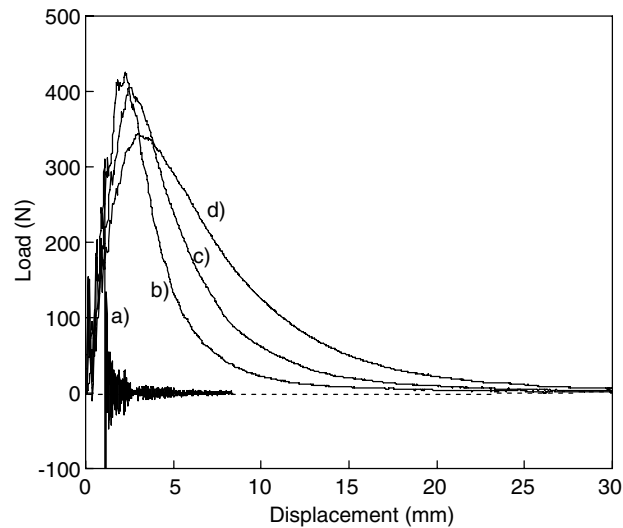
Fig. 5. Load–displacement curves under Charpy impact conditions for (a) neat, (b) 7 wt% rubber modified, (c) 16 wt% rubber modified, and (d) 25 wt% rubber modified polyamide-66. Specimens conditioned at $T = 21$ °C and RH $= 30$%.

Table 2
Charpy impact data of neat and rubber modified polyamide-66

Rubber content (wt%)	Charpy impact strength (kJ/m^2)	Maximum load (N)	Ductility index
0	4.5 ± 0.2	304 ± 24	0.08
7	55.5 ± 2.3	428 ± 13	2.44
16	73.9 ± 1.2	402 ± 8	3.19
25	94.5 ± 0.4	346 ± 2	3.46

where $w_{e,init}$ and $w_{e,prop}$ represent the components of the specific essential work of fracture related to the crack-initiation and crack-propagation, respectively, such as

$$w_e = w_{e,init} + w_{e,prop} \tag{8}$$

By way of example, the load displacement curves of polyamide-66 DDENT specimens at various ligament lengths tested at a cross-head speed of 10 mm/min are reported in Fig. 7a. The self-similarity of the curves, which is a major requirement for the validity of the EWF approach, is quite satisfactory. Accordingly to Eqs. (5) and (7), the data reduction of the experimental points remaining after the application of the criteria of the test protocol (see Section 2) yields plots such as those reported in Fig. 7b. The intercepts of the linear regression lines allowed us to determine the parameter w_e along with its components $w_{e,init}$ and $w_{e,prop}$.

3.2.2. Effect of moisture content

It is well known that polyamides absorb water reversibly, and that it usually acts as a plasticizer with a beneficial effect on their fracture toughness but with a considerable loss in the elastic and ultimate properties [49,63,64]. The effect of moisture content on the load–displacement curves of neat polyamide-66 DDENT specimens with the same ligament length but different moisture contents is evidenced in Fig. 8 for samples tested at a cross-head speed of 10 mm/min. It is interesting to observe that in the dry state the specimens behave in a completely brittle manner (curve a) without any yield phenomena. The specimens in equilibrium with the laboratory humidity (curve b) contain 1.3 wt% moisture and show a completely ductile behaviour with yielding and subsequent crack propagation. The specimens conditioned in hot water up to a moisture content of 9.3 wt% show a ductile behaviour with a much lower value of the maximum load and a simultaneous increase of the elongation at break. The consequences of this behaviour on the EWF parameters are summarized in Fig. 9. First of all, it is important to note that for the dry sample the EWF approach is not strictly applicable, since it requires complete
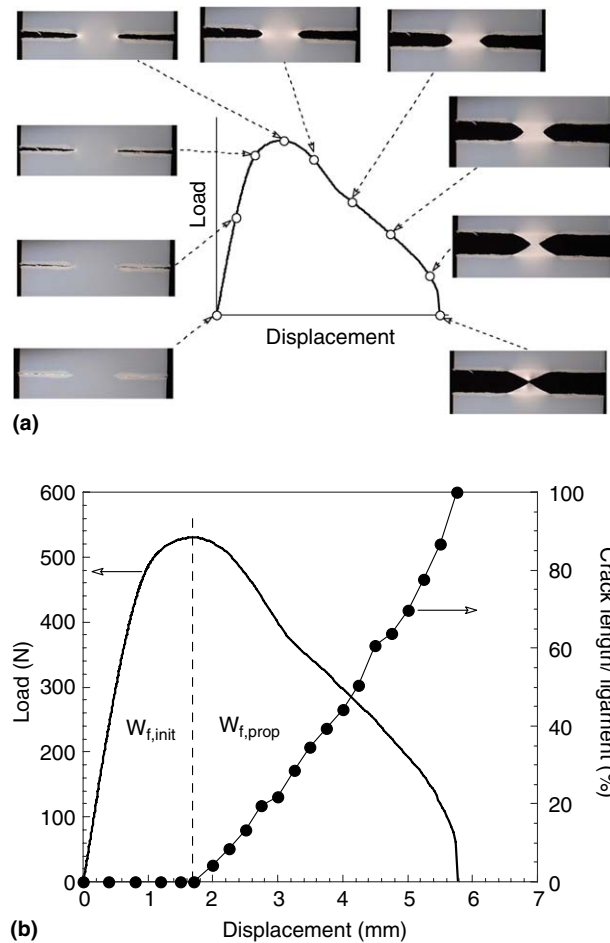
Fig. 6. Load–displacement curve for neat polyamide-66 DDENT specimen with a moisture content is 1.3 wt% tested at a cross-head speed of 10 mm/min: (a) photograms of the fracture process, (b) evolution of the crack length during the fracture test.

ligament yielding prior to crack propagation. Anyway, for sake of comparison we still report under round brackets the parameters obtained according to the EWF data reduction approach for the dry sample, even if they could be more appropriately interpreted in the framework of a linear elastic fracture mechanics approach. In Fig. 9a it is interesting to note that the specific essential work of fracture values increase as the sample moisture content increases. The specific non-essential term βw_p associated to the plastic deformation in the outer process zone is practically zero for the dry sample and substantially independent of the moisture content in the investigated range. The partitioning of the w_e into its crack initiation $w_{e,init}$ and crack propagation $w_{e,prop}$ components gives a further insight into the effect of moisture on the fracture behaviour of neat polyamide-66. In fact, as reported in Fig. 9b, the toughening effect due to moisture can be almost entirely attributed to an increase in the specific essential work of fracture component related to the crack propagation process, the crack initiation component being practically unaffected by the moisture content.

3.2.3. Effect of rubber content

The effect of rubber content on the load–displacement curves of DDENT specimens with the same ligament length is shown in Fig. 10 for a cross-head speed of 10 mm/min. It is evident that the maximum load (and hence the maximum net-section stress) decreases as the rubber content increases. On the other hand, the maximum elongation observed for DDENT specimens is practically unaffected by the rubber content, even if both the strain at yield ad strain at break values obtained in tensile tests show a certain tendency to increase with the
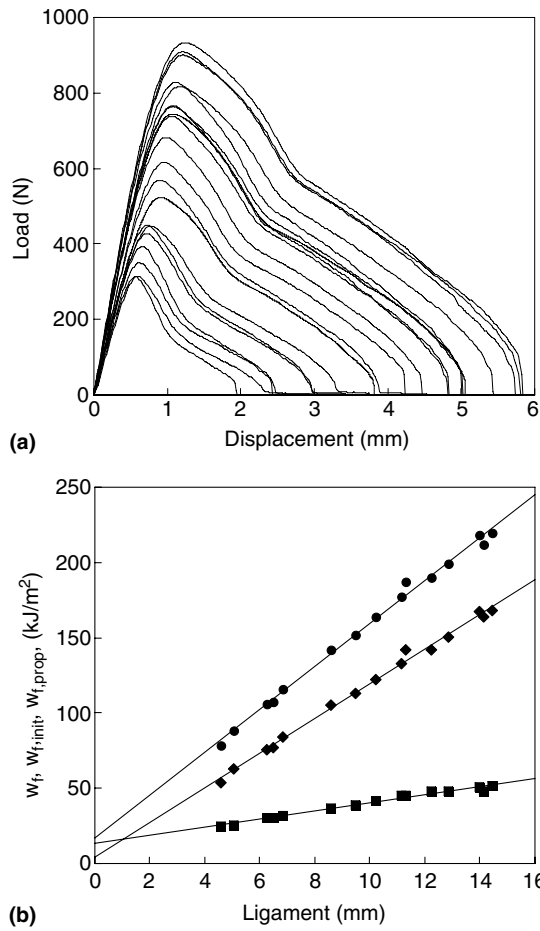
Fig. 7. Polyamide-66 DDENT specimens with a moisture content of 1.3 wt% and various ligament lengths tested at a cross-head speed of 10 mm/min: (a) load–displacement curves, (b) total specific work of fracture w_f (●), specific work for crack initiation $w_{f,init}$ (■) and specific work for crack propagation $w_{f,prop}$ (◆) against ligament length.
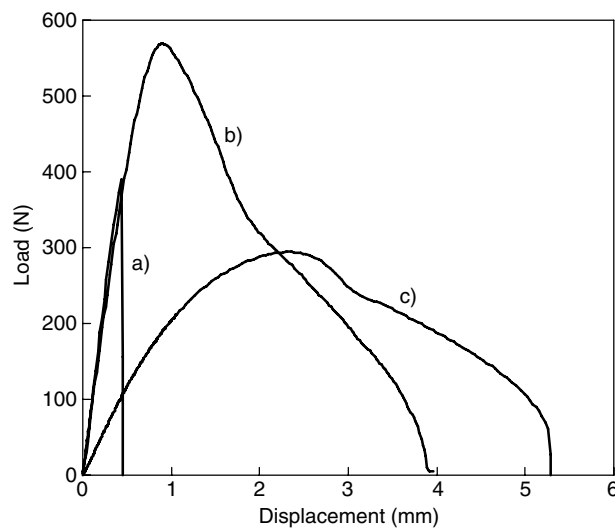
Fig. 8. Load–displacement curves for DDENT specimens with the same ligament length ($L = 8.6$ mm) at a cross-head speed of 10 mm/min for neat polyamide-66 DDENT at various moisture contents: (a) dry, (b) 1.3 wt%, (c) 9.3 wt%.
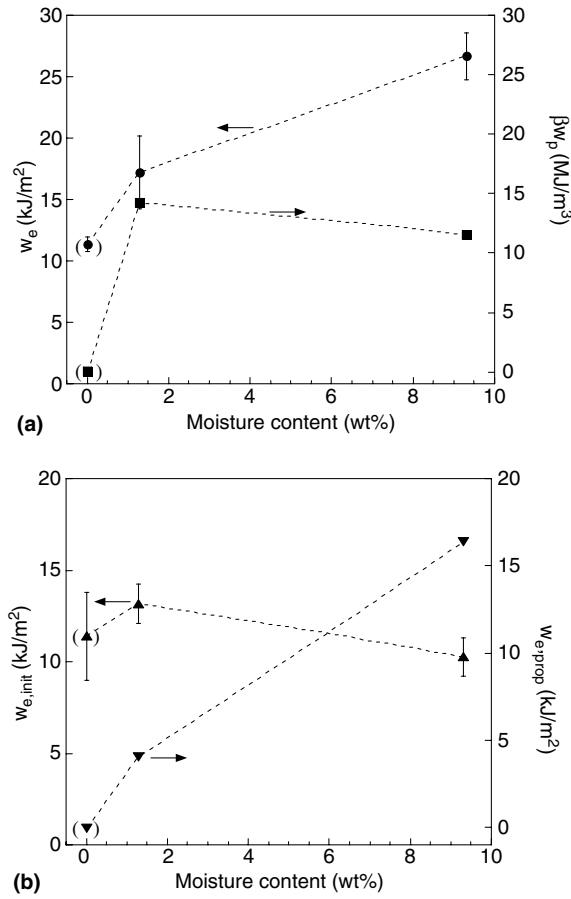
Fig. 9. Effect of moisture content on the EWF values of polyamide-66 tested at a cross-head speed of 10 mm/min. Values refer to (a) the essential w_e (●) and non-essential βw_p (■) specific work of fracture, and (b) the specific work of fracture for crack initiation $w_{e,init}$ (▲) and for crack propagation $w_{e,prop}$ (▼), respectively.
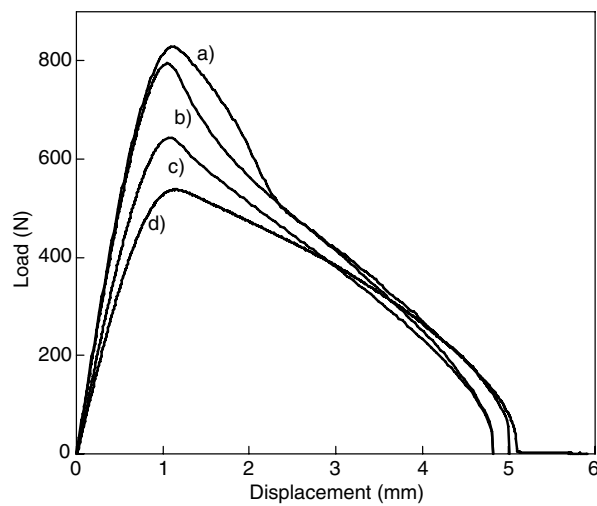
Fig. 10. Load–displacement curves for DDENT specimens with the same ligament length ($L = 12$ mm) at a cross-head speed of 10 mm/min for (a) neat, (b) 7 wt% rubber modified, (c) 16 wt% rubber modified, and (d) 25 wt% rubber modified polyamide-66. Specimens conditioned at $T = 21$ °C and RH = 30%.
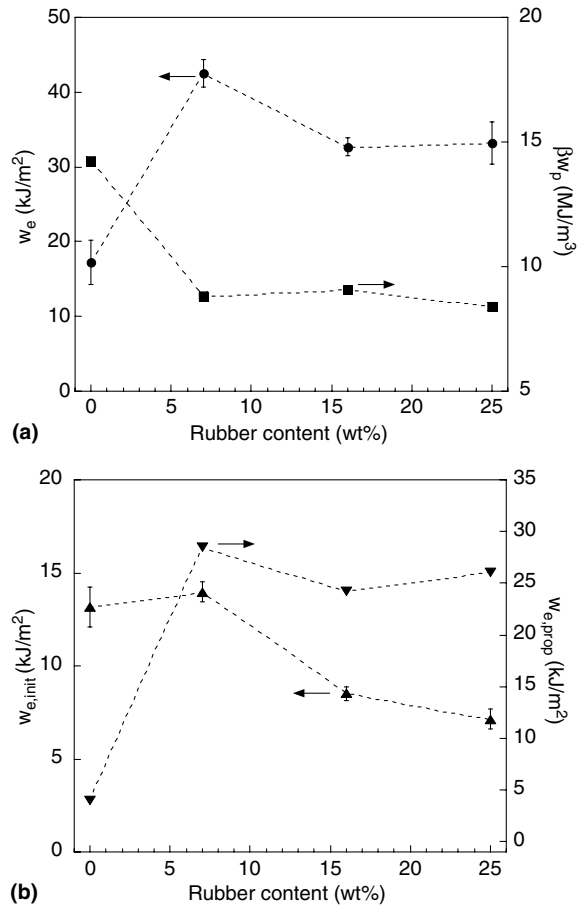
Fig. 11. Effect of rubber content on the EWF values of polyamide-66 tested at a cross-head speed of 10 mm/min. Values refer to (a) the essential w_e (●) and non-essential βw_p (■) specific work of fracture, and (b) the specific work of fracture for crack initiation $w_{e,init}$ (▲) and for crack propagation $w_{e,prop}$ (▼), respectively. Specimens conditioned at $T = 21\ °C$ and RH = 30%.
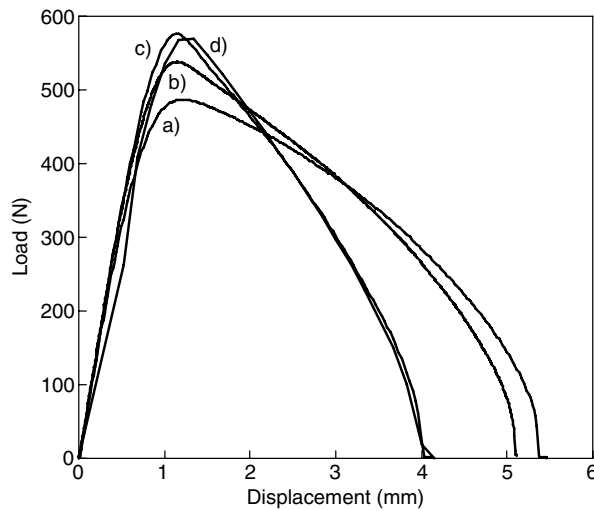
Fig. 12. Load–displacement curves for DDENT specimens of 25 wt% rubber modified polyamide-66 with the same ligament length ($L = 12$ mm) tested at the cross-head speeds of (a) 1 mm/min, (b) 10 mm/min, (c) 100 mm/min, and (d) 500 mm/min. Specimens conditioned at $T = 21\ °C$ and RH = 30%.

rubber content (see Fig. 4b and c). The effect of the rubber content on the EWF parameters is summarized in Fig. 11. First of all, it is worthwhile to note that the rubber toughened materials display specific essential work of fracture values much higher that the neat polyamide-66 matrix. On the other hand this wide increase in w_e parameter seems to be not directly proportional to the rubber content since w_e values pass trough a maximum for a rubber content of 7 wt% and tends to a lower but constant value for higher rubber contents. Therefore, the effect of rubber content on the plane-stress fracture toughness at low loading rates substantially differs from the trend observed for Charpy impact resistance (see Table 2). Beside the differences in the test configurations, these experimental evidences are in good agreement with the observations of Dijkstra et al. [12]. They performed instrumented notched tensile impact tests of nylon-6/(ethylene–propylene rubber) blends over a broad range of testing speeds (including strain rates encountered in normal tensile tests and in impact tests). They observed that the effect of rubber content on the total fracture energy markedly depends on the testing speed, only for the highest speed (impact) being a higher rubber content beneficial for a high fracture energy. For low and intermediate testing speeds a low rubber concentration is already sufficient for toughening polyamide-6. The sudden rise in fracture energy with rising strain rate is believed to be caused by a transition from isothermal to adiabatic deformation [12]. In the adiabatic regime the rise in temperature is high enough to melt the material around the crack tip, as confirmed by SEM studies of the deformation zone [12]. Interestingly enough, the data reported in
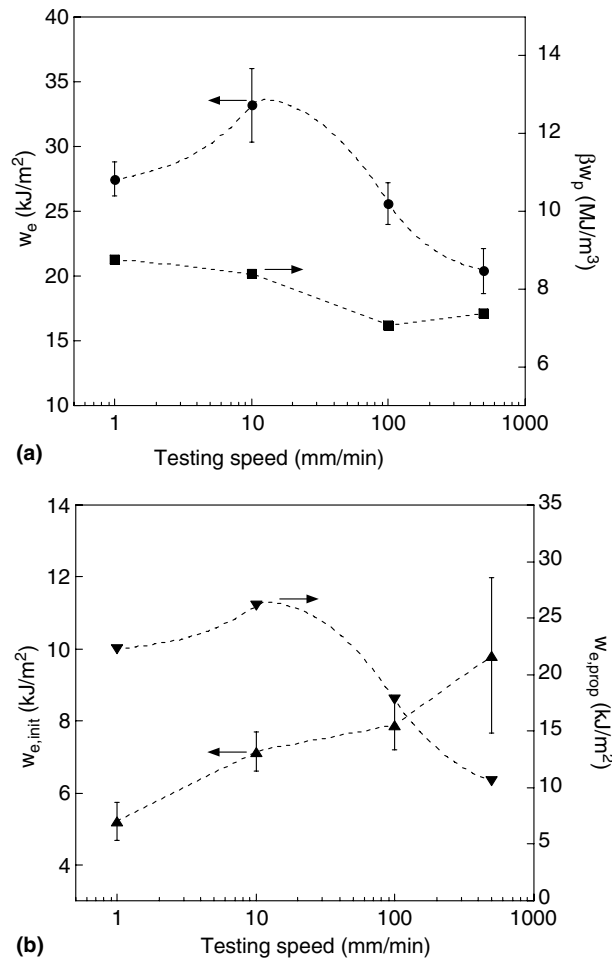
Fig. 13. Effect of testing speed on the EWF values of 25 wt% rubber modified polyamide-66. Values refer to (a) the essential w_e (●) and non-essential βw_p (■) specific work of fracture, and (b) the specific work of fracture for crack initiation $w_{e,init}$ (▲) and for crack propagation $w_{e,prop}$ (▼), respectively. Specimens conditioned at $T = 21$ °C and RH = 30%.

Fig. 11a indicate that the non-essential specific work of fracture parameter of rubber toughened polyamide-66 is lower than that of the neat polymer matrix and practically independent of the rubber content.

The specific essential work of fracture terms related to fracture initiation and crack-propagation display different trends with the rubber content as depicted in Fig. 11b. In fact, as the rubber content increases, the term $w_{e,init}$ slightly decreases while the term $w_{e,prop}$ initially increases and then remains practically constant. The higher value of the specific essential work of fracture parameter of the 7 wt% rubber toughened material is hence related to a favourable compromise between its fracture initiation and propagation components.

3.2.4. Effect of strain rate

The effect of strain rate on the work of fracture parameters has been investigated on the 25 wt% rubber toughened polyamide-66 sample. As evidenced in Fig. 12, as the strain rate increases the load–displacement curves of DDENT specimens display slightly higher values of the maximum load and a tendency for the elongation at break to decrease. As summarized in Fig. 13a, the specific essential work of fracture parameter passes through a maximum for a cross-head speed of 10 mm/min and then it decreases, while the specific non-essential work of fracture term is practically independent of the testing speed. As reported in Fig. 13b, the trend of the w_e parameter is the result of two contributions, $w_{e,init}$ and $w_{e,prop}$, that are affected by the strain rate in quite different ways. In fact, the term related to crack initiation increases with the testing speed, while, at the same time, the term associated to crack propagation shows a tendency to decrease. This opposite trends for the strain rate dependence of $w_{e,init}$ and $w_{e,prop}$ components is not peculiar to this material but it has been also observed for many other ductile polymeric materials such as semi-crystalline poly(ethylene-terephthalate) [56], poly(ethylene-naphthalate) [59], nylon-6 [65], unplasticized poly(vinyl chloride) [52,62], isotactic polypropylene [53,60,61,65], and linear low-density-polyethylene/butene copolymer [65].

4. Conclusions

The EWF approach has been applied to study the fracture behaviour of neat and rubber toughened polyamide-66. The following conclusions can be drawn:

  (i) Tests performed on neat polyamide-66 specimens conditioned up to various equilibrium moisture contents clearly indicate that w_e markedly increases as the material moisture content rises, and that this trend is mainly associated with the increase of its crack propagation component ($w_{e,prop}$), the initiation related term ($w_{e,init}$) being practically independent of the humidity level.
 (ii) The inclusion of various amounts (7, 16, and 25 wt%) of rubber particles into the polyamide-66 matrix induces a large increase of the w_e parameter with $w_{e,init}$ and $w_{e,prop}$ terms displaying different trends with the rubber content. Most of the toughening effect of the rubber particles can be attributed to a large increase of the propagation-related term, the fracture initiation term decreasing with the rubber content.
(iii) The loading rate effects on the fracture behaviour have been investigated on polyamide-66 toughened with 25 wt% rubber. An increase of the loading rate causes an increase of the crack-initiation related term $w_{e,init}$, while the crack-propagation related parameter $w_{e,prop}$ decreases. As a consequence, the specific term w_e shows a non-monotonic trend with the loading rate.

References

[1] Bucknall CB. Toughened plastics. London: Applied Science Ltd; 1977.
[2] Collyer AA, editorRubber toughened engineering plastics. London: Chapmann & Hall; 1994.

[3] Kinloch AJ, Young RJ. Fracture behaviour of polymers. London: Applied Science Ltd; 1983.

[4] Lazzeri A, Bucknall CB. Dilatational bands in rubber-toughened polymers. J Mater Sci 1993;28(24):6799–808.

[5] Kohan MI, editor. Nylon plastics handbook. Munich: Hanser Publishers; 1995.

[6] Wu S. Phase structure and adhesion in polymer blends: a criterion for rubber toughening. Polymer 1985;26:1855–63.

[7] Cimmino S, Coppola F, D'Orazio L, Greco R, Maglio G, Malinconico M, et al. Ternary nylon-6/rubber/modified rubber blends: effect of the mixing procedure on morphology, mechanical and impact properties. Polymer 1986;27:1874–84.

[8] Borggreve RJM, Gaymans RJ, Schuijer J, Ingen Housz JF. Brittle-tough transition in nylon–rubber blends: effect of rubber concentration and particle size. Polymer 1987;28:1489–96.

[9] Ricco T, Pavan A. Fracture mechanics analysis of rubber-modified polyamide-6: temperature and rate effects with varying rubber content. Angew Makromol Chem 1992;201:23–31.

[10] Wu CJ, Ku JF, Chen CY. Rubber-toughened polyamide-6—the influence of compatibilizer on morphology and impact properties. Polym Eng Sci 1993;33(20):1329–35.

[11] Dijkstra K, Gaymans RJ. Nylon-6 rubber blends. 8. Influence of the molecular-weight of the matrix on the impact behavior. Polymer 1994;35(2):332–5.

[12] Dijkstra K, Terlaak J, Gaymans RJ. Nylon-6 rubber blends. 6. Notched tensile impact testing of nylon-6/(ethylene–propylene rubber) blends. Polymer 1994;35(2):315–22.

[13] Lu M, Keskkula HG, Paul DR. Toughening of nylon 6 with grafted rubber impact modifiers. J Appl Polym Sci 1995;58(7):1175–88.

[14] Muratoglu OK, Argon AS, Cohen RE, Weinberg M. Toughening mechanism of rubber-modified polyamides. Polymer 1995;36(5):921–30.

[15] Lu M, Keskkula HG, Paul DR. Toughening of nylon 6 with core–shell impact modifiers: effect of matrix molecular weight. J Appl Polym Sci 1996;59(9):1467–77.

[16] Oshinski AJ, Keskkula H, Paul DR. The role of matrix molecular weight in rubber toughened nylon 6 blends.1. Morphology. Polymer 1996;37(22):4891–907.

[17] Burgisi G, Paternoster M, Peduto N, Saraceno A. Toughness enhancement of polyamide 6 modified with different types of rubber: the influence of internal rubber cavitation. J Appl Polym Sci 1997;66(4):777–87.

[18] Kayano Y, Keskkula H, Paul DR. Fracture behaviour of some rubber-toughened nylon 6 blends. Polymer 1998;39(12):2835–45.

[19] Okada O, Keskkula H, Paul DR. Fracture toughness of nylon 6 blends with maleated ethylene/propylene rubbers. Polymer 2000;41:8061–74.

[20] Lievana E, Bernal C, Frontini P. Essential work of fracture of rubber-modified polyamide 6 in impact. Polym Eng Sci 2004;44(9):1707–15.

[21] Okada O, Keskkula H, Paul DR. Fracture toughness of nylon-6 blends with maleated rubbers. J Polym Sci, Part B: Polym Phys 2004;42(9):1739–58.

[22] Gaymans RJ. Toughened polyamides. In: Collyer AA, editor. Rubber toughened engineering plastics. London: Chapmann & Hall; 1994. p. 210–42.

[23] Keskkula H, Paul DR. Toughened nylons. In: Kohan MI, editor. Nylon plastics handbook. Munich: Hanser Publishers; 1995. p. 414–434.

[24] Hashemi S, Williams JG. Single and multi-specimens *R*-curve methods for JIC determination of toughened nylons. J Mater Sci 1991;26(3):621–30.

[25] Crounch BA, Huang DD. The *J*-integral technique applied to toughened nylons under impact loading. J Mater Sci 1994;29(4):861–4.

[26] Williams JG. Introduction to linear elastic fracture mechanics. In: Moore DR, Pavan A, Williams JG, editors. Fracture mechanics testing methods for polymers, adhesives and composites. Amsterdam: Elsevier; 2001. p. 3–10.

[27] Standard ASTM D5045-99. Plane-strain fracture toughness and strain energy release rate of plastic materials.

[28] Standard ISO 13586:2000. Plastics—determination of fracture toughness (GIC and KIC)—linear elastic fracture mechanics (LEFM) approach.

[29] Williams JG. Introduction to elastic–plastic fracture mechanics. In: Moore DR, Pavan A, Williams JG, editors. Fracture mechanics testing methods for polymers adhesives and composites. Amsterdam: Elsevier; 2001. p. 119–22.

[30] Standard ASTM D6068-96. Determining *J–R* curves of plastic materials.

[31] Hale GE, Ramsteiner F. *J*-Fracture toughness of polymers at slow speed. In: Moore DR, Pavan A, Williams JG, editors. Fracture mechanics testing methods for polymers, adhesives and composites. Amsterdam: Elsevier; 2001. p. 123–57.

[32] Clutton E. Essential work of fracture. In: Moore DR, Pavan A, Williams JG, editors. Fracture mechanics testing methods for polymers adhesives and composites. Amsterdam: Elsevier; 2001. p. 177–95.

[33] Mai YW, Cotterell B. On the essential work of ductile fracture in polymers. Int J Fract 1986;32:105–25.

[34] Chan WY, Williams JG. Determination of the fracture toughness of polymeric films by the essential work method. Polymer 1994;35(8):1666–72.

[35] Yamakawa RS, Razzino CA, Correa CA, Hage Jr E. Influence of notching and molding conditions on determination of EWF parameters in polyamide 6. Polym Test 2004;23(2):195–202.

[36] Laura DM, Keskkula H, Barlow JW, Paul DR. Effect of glass fiber and maleated ethylene–propylene rubber content on tensile and impact properties of nylon 6. Polymer 2000;41(19):7165–74.

[37] Cho JW, Paul DR. Glass fiber-reinforced polyamide composites toughened with ABS and EPR-g-MA. J Appl Polym Sci 2001;80(3):484–97.

[38] Laura DM, Keskkula H, Barlow JW, Paul DR. Effect of glass fiber and maleated ethylene–propylene rubber content on the impact fracture parameters of nylon 6. Polymer 2001;42(14):6161–72.

[39] Karayannidis GP, Bikiaris DN, Papageorgiou GZ, Bakirtzis V. Rubber toughening of glass fiber reinforced nylon-6,6 with functionalized block copolymer SEBS-g-MA. Adv Polym Techn 2002;21(3):153–63.

[40] Wong SC, Sui GX, Yue CY, Mai YW. Characterization of microstructures and toughening behavior of fiber-containing toughened nylon 6,6. J Mater Sci 2002;37(13):2659–67.

[41] Ching ECY, Li RKY, Tjong SC, Mai YW. Essential work of fracture (EWF) analysis for short glass fiber reinforced and rubber toughened nylon-6. Polym Eng Sci 2003;43(3):558–69.

[42] Laura DM, Keskkula H, Barlow JW, Paul DR. Effect of rubber particle size and rubber type on the mechanical properties of glass fiber reinforced, rubber-toughened nylon 6. Polymer 2003;44(11):3347–61.

[43] Tjong SC, Xu SA, Mai YW. Impact fracture toughness of short glass fiber-reinforced polyamide 6,6 hybrid composites containing elastomer particles using essential work of fracture concept. Mater Sci Eng, A 2003;347(1-2):338–45.

[44] Tjong SC, Bao SP. Impact fracture toughness of polyamide-6/montmorillonite nanocomposites toughened with a maleated styrene/ethylene butylene/styrene elastomer. J Polym Sci, Part B: Polym Phys 2005;43:585–95.

[45] Data sheets available from <http://www.radiciplastics.com> [Last access February 2006].

[46] Standard ISO 527-2:1993. Plastics—determination of tensile properties—Part 2: Test conditions for moulding and extrusion plastics.

[47] Standard ISO 179-2:1997. Plastics—Determination of Charpy impact properties—Part 2: Instrumented impact test.

[48] McCrum NG. Anelastic and dielectric effects in polymeric solids. New York: Dover; 1984.

[49] Mohd Ishak ZA, Perry JP. Effect of moisture absorption on the dynamic-mechanical properties of short carbon–fiber-reinforced nylon 6,6. Polym Comp 1995;15(3):223–30.

[50] Beaumont PWR, Reiwald PG, Zweben C. Methods for improving the impact resistance of composite materials. ASTM Spec Tech Publ 1974;568:134–58.

[51] Karger-Kocsis J, Czigany T, Moskala EJ. Thickness dependence of work of fracture parameters of an amorphous copolyester. Polymer 1997;38:4587–93.

[52] Arkhireyeva A, Hashemi S, O'Brien M. Factors affecting work of fracture of uPVC film. J Mater Sci 1999;34:5961–74.

[53] Ferrer-Balas D, Maspoch ML, Martinez AB, Santana OO. On the essential work of fracture method: energy partitioning of the fracture process in iPP films. Polym Bull 1999;42:101–8.

[54] Hashemi S, Williams JG. Temperature dependence of essential and non-essential work of fracture parameters for polycarbonate film. Plastic, Rubber Compos 2000;29(6):294–302.

[55] Barany T, Karger-Kocsis J, Czigány T. Effect of hygrothermal aging on the essential work of fracture response of amorphous poly(ethylene terephthalate) sheets. Polym Degrad Stab 2003;82(2):271–8.

[56] Pegoretti A, Ricco T. Rate and temperature effects on the plane stress essential work of fracture in semicrystalline PET. In: Blackman BRK, Pavan A, Williams JG, editors. Fracture of polymers, composites and adhesives II. Amsterdam: Elsevier; 2003. p. 89–100.

[57] Arkhireyeva A, Hashemi S. Effect of temperature on work of fracture parameters in poly(ether-ether ketone) (PEEK) film. Eng Fract Mech 2004;71(4-6):789–804.

[58] Barany T, Karger-Kocsis J. In-plane fracture toughness of PET fiber-reinforced paper as a function of UV-irradiation. J Macromol Sci, Phys 2004;B43(3):671–83.

[59] Karger-Kocsis J, Czigany T. Strain rate dependence of work of fracture response of an amorphous poly(ethylene-naphthalate) (PEN) film. Polym Eng Sci 2000;40(8):1809–15.

[60] Karger-Kocsis J, Barany T. Plane-stress fracture behaviour of syndiotactic polypropylenes of various crystallinity as assessed by the essential work of fracture method. Polym Eng Sci 2002;42(7):1410–9.

[61] Grein C, Plummer CJG, Germain Y, Kausch HH, Beguelin P. Essential work of fracture of polypropylene and polypropylene blends over a wide range of test speeds. Polym Eng Sci 2003;43:223–33.

[62] Maspoch ML, Gamez-Perez J, Karger-Kocsis J. Effects of thickness, deformation rate and energy partitioning on the work of fracture parameters of uPVC films. Polym Bull 2003;50:279–86.

[63] Williams JCL, Watson SJ, Boydell P. Properties. In: Kohan MI, editor. Nylon plastics handbook. Munich: Hanser Publishers; 1995. p. 293–358.

[64] Huang JC, Yang ZY, Grossman SJ. Effects of moisture on mechanical properties of rubber-modified nylon-6,6. J Polym Eng 1999;19(5):305–14.

[65] Pegoretti A, Ricco T. Plane stress ductile fracture of some polymeric films under quasi-static and impact conditions: essential work of fracture approach, in preparation.